J Electr Eng Technol Vol. 9, No. 6: 1882-1890, 2014
http://dx.doi.org/10.5370/JEET.2014.9.6.1882

ISSN(Print) 1975-0102
ISSN(Online) 2093-7423

Multi-Objective Short-Term Fixed Head Hydrothermal Scheduling Using Augmented Lagrange Hopfield Network

Thang Trung Nguyen† and Dieu Ngoc Vo*

Abstract – This paper proposes an augmented Lagrange Hopfield network (ALHN) based method for solving multi-objective short term fixed head hydrothermal scheduling problem. The main objective of the problem is to minimize both total power generation cost and emissions of NO_x, SO_2, and CO_2 over a scheduling period of one day while satisfying power balance, hydraulic, and generator operating limits constraints. The ALHN method is a combination of augmented Lagrange relaxation and continuous Hopfield neural network where the augmented Lagrange function is directly used as the energy function of the network. For implementation of the ALHN based method for solving the problem, ALHN is implemented for obtaining non-dominated solutions and fuzzy set theory is applied for obtaining the best compromise solution. The proposed method has been tested on different systems with different analyses and the obtained results have been compared to those from other methods available in the literature. The result comparisons have indicated that the proposed method is very efficient for solving the problem with good optimal solution and fast computational time. Therefore, the proposed ALHN can be a very favorable method for solving the multi-objective short term fixed head hydrothermal scheduling problems.

Keywords: Augmented lagrange hopfield network, Fixed head, Fuzzy set theory, Hydrothermal scheduling, Multi-objective

1. Introduction

The short term hydro-thermal scheduling (HTS) problem is to determine power generation among the available thermal and hydro power plants so that the fuel cost of thermal units is minimized over a schedule time of a single day or a week while satisfying both hydraulic and electrical operational constraints such as the quantity of available water, limits on generation, and power balance [1]. However, the major amount electric power in power systems is produced by thermal plants using fossil fuel such as oil, coal, and natural gases [2]. In fact, the process of electricity generation from fossil fuel releases several contaminants such as nitrogen oxides (NO_x), sulphur dioxide (SO_2), and carbon dioxide (CO_2) into the atmosphere [3]. Therefore, the HTS problem can be extended to minimize the gaseous emission as a result of the recent environmental requirements in addition to the minimization the fuel cost of thermal power plants, forming the multi-objective HTS problem. The multi-objective HTS problem is more complex than the HTS problem since it needs to find several obtained non-dominated solutions to determine the best compromise solution which leads to time consuming. Therefore, the solution methods for the multi-objective HTS have to be efficient and effective for obtaining optimal solutions.

In the past decades, several conventional methods have been used to solve the classical HTS problem neglecting environment aspects such as dynamic programming (DP) [4], network flow programming (NFP) [5], Lagrange relaxation (LR) [6], and Benders decomposition [7] methods. Among these methods, the DP and LR methods are more popular ones. However, the computational and dimensional requirements of the DP method increase drastically with large-scale system planning horizon which is not appropriate for dealing with large-scale problems. On the contrary, the LR method is more efficient and can deal with large-scale problems. However, the solution quality of the LR for optimization problems depends on its duality gap which results from the dual problem formulation and might oscillate, leading to divergence for some problems with operation limits and non-convexity of incremental heat rate curves of generators. The Benders decomposition method is usually used to reduce the dimension of the problem into subproblems which can be solved by DP, Newton's, or LR method. In addition to the conventional methods, several artificial intelligence based methods have been also implemented for solving the HTS problem such as simulated annealing (SA) [8], evolutionary programming (EP) [9], genetic algorithm (GA) [10], differential evolution (DE) [11], and particle swarm optimization (PSO) [12]. These methods can find a near optimum solution for a complex problem. However, these metaheuristic search methods are based on a

† Corresponding Author: Dept. of Electrical and Electronics Engineering, Ton Duc Thang University, Vietnam. (trungthangttt@tdt.edu.vn)
* Dept. of Power Systems, Ho Chi Minh City University of Technology, Vietnam. (vndieu@gmail.com)
Received: March 4, 2013; Accepted: July 24, 2014

population for searching an optimal solution, leading to time consuming for large-scale problems. More, these methods need to be run several times to obtain an optimal solution which is not appropriate for obtaining several non-dominated solution for a multi-objective optimization problem. Recently, neural networks have been implemented for solving optimization problem in hydrothermal systems such as two-phase neural network [13], combined Hopfield neural network and Lagrange function (HLN) [14], and combined augmented Lagrange function with Hopfield neural network [15-17]. The advantage of the neural networks is fast computation using parallel processing. Moreover, the Hopfield neural network based on the Lagrange function can also overcome other drawbacks of the conventional Hopfield network in finding optimal solutions for optimization problems such as easy implementation and global solution. Therefore, the neural networks are more appropriate for solving multi-objective optimization problems with several solutions determined for each problem.

In this paper, an augmented Lagrange Hopfield network (ALHN) based method is proposed for solving multi-objective short term fixed head HTS problem. The main objective of the problem is to minimize both total power generation cost and emissions of NO_x, SO_2, and CO_2 over a scheduling period of one day while satisfying power balance, hydraulic, and generator operating limits constraints. The ALHN method is a combination of augmented Lagrange relaxation and continuous Hopfield neural network where the augmented Lagrange function is directly used as the energy function of the network. For implementation of the ALHN based method for solving the problem, ALHN is implemented for obtaining non-dominated solutions and fuzzy set theory is applied for obtaining the best compromise solution. The proposed method has been tested on different systems with different analyses and the obtained results have been compared to those from other methods available in the literature including λ-γ iteration method (LGM), existing PSO-based HTS (EPSO), and PSO based method (PM) in [3] and bacterial foraging algorithm (BFA) [2].

The organization of this paper is as follows. Section 2 addresses the multi-objective HTS problem formulation. The proposed ALHN based method is described in Section 3. Numerical results are presented in Section 4. Finally, the conclusion is given.

2. Problem Formulation

The main objective of the economic emission dispatch for the HTS problem is to minimize the total fuel cost and emissions of all thermal plants while satisfying all hydraulic, system, and unit constraints. Mathematically, the fixed-head short-term hydrothermal scheduling problem including N_1 thermal plants and N_2 hydro plants scheduled in M sub-intervals is formulated as follows:

$$MinC_T = \sum_{k=1}^{M}\sum_{s=1}^{N_1} t_k\left(w_1F_{1sk} + w_2F_{2sk} + w_3F_{3sk} + w_4F_{4sk}\right) \quad (1)$$

$$F_{1sk} = \left(a_{1s} + b_{1s}P_{sk} + c_{1s}P_{sk}^2\right) \ \text{\$/h} \quad (2)$$

$$F_{2sk} = \left(d_{1s} + e_{1s}P_{sk} + f_{1s}P_{sk}^2\right) \ \text{kg/h} \quad (3)$$

$$F_{3sk} = \left(d_{2s} + e_{2s}P_{sk} + f_{2s}P_{sk}^2\right) \text{kg/h} \quad (4)$$

$$F_{4sk} = \left(d_{3s} + e_{3s}P_{sk} + f_{3s}P_{sk}^2\right) \text{kg/h} \quad (5)$$

$$\sum_{i=1}^{4} w_i = 1 \quad (6)$$

where F_{1sk} is fuel cost function; F_{2sk}, F_{3sk} and F_{4sk} are emission function of NO_x, SO_2, and CO_2 of sth thermal plant at kth sub-interval scheduling, respectively; w_i (i = 1, …, 4) are weights corresponding to the objectives.

subject to:

Power balance constraints:

$$\sum_{s=1}^{N_1} P_{sk} + \sum_{h=1}^{N_2} P_{hk} - P_{Lk} - P_{Dk} = 0 \ ; \ k = 1,\ldots, M \quad (7)$$

$$P_{Lk} = \sum_{i=1}^{N_1+N_2}\sum_{j=1}^{N_1+N_2} P_{ik}B_{ij}P_{jk} + \sum_{i=1}^{N_1+N_2} B_{0i}P_{ik} + B_{00} \quad (8)$$

where B_{ij}, B_{0i}, and B_{00} are loss formula coefficients of transmission system.

Water availability constraints:

$$\sum_{k=1}^{M} t_k\left(q_{hk} - r_{hk}\right) = W_h \quad (9)$$

where $$q_{hk} = a_h + b_hP_{hk} + c_hP_{hk}^2 \quad (10)$$

Generator operating limits:

$$P_s^{\min} \le P_{sk} \le P_s^{\max} \ ; \ s = 1, \ldots, N_1; \ k = 1, \ldots, M \quad (11)$$

$$P_h^{\min} \le P_{hk} \le P_h^{\max} \ ; \ h = 1, \ldots, N_2; \ k = 1, \ldots, M \quad (12)$$

3. ALHN based Method for the Problem

3.1 ALHN for optimal solutions

For implementation of the proposed ALHN for finding optimal solution of the problem, the augmented Lagrange function is firstly formulated and then this function is used as the energy function of conventional Hopfield neural network. The model of ALHN is solved using gradient method.

The augmented Lagrange function L of the problem is formulated as follows:

$$
\begin{aligned}
L = & \sum_{k=1}^{M}\sum_{s=1}^{N_1} t_k\left(a_s + b_s P_{sk} + c_s P_{sk}^2\right) \\
& + \sum_{k=1}^{M}\lambda_k\left(P_{Lk} + P_{Dk} - \sum_{s=1}^{N_1}P_{sk} - \sum_{h=1}^{N_2}P_{hk}\right) \\
& + \sum_{h=1}^{N_2}\gamma_h\left[\sum_{k=1}^{M}t_k\left(q_{hk} - r_{hk}\right) - W_h\right] \\
& + \frac{1}{2}\sum_{k=1}^{M}\beta_k\left(P_{Lk} + P_{Dk} - \sum_{s=1}^{N_1}P_{sk} - \sum_{h=1}^{N_2}P_{hk}\right)^2 \\
& + \frac{1}{2}\sum_{h=1}^{N_2}\beta_h\left[\sum_{k=1}^{M}t_k\left(q_{hk} - r_{hk}\right) - W_h\right]^2
\end{aligned} \tag{13}
$$

where λ_k and γ_h are Lagrangian multipliers associated with power balance and water constraints, respectively; β_k, β_h are penalty factors associated with power balance and water constraints, respectively; and

$$a_s = w_1 a_{1s} + w_2 d_{1s} + w_3 d_{2s} + w_4 d_{3s} \tag{14}$$

$$b_s = w_1 b_{1s} + w_2 e_{1s} + w_3 e_{2s} + w_4 e_{3s} \tag{15}$$

$$c_s = w_1 c_{1s} + w_2 f_{1s} + w_3 f_{2s} + w_4 f_{3s} \tag{16}$$

The energy function E of the problem is described in terms of neurons as follows:

$$
\begin{aligned}
E = & \sum_{k=1}^{M}\sum_{s=1}^{N_1} t_k\left(a_s + b_s V_{sk} + c_s V_{sk}^2\right) \\
& + \sum_{k=1}^{M}V_{\lambda k}\left(P_{Lk} + P_{Dk} - \sum_{s=1}^{N_1}V_{sk} - \sum_{h=1}^{N_2}V_{hk}\right) \\
& + \sum_{h=1}^{N_2}V_{\gamma h}\left[\sum_{k=1}^{M}t_k\left(q_{hk} - r_{hk}\right) - W_h\right] \\
& + \frac{1}{2}\sum_{k=1}^{M}\beta_k\left(P_{Lk} + P_{Dk} - \sum_{s=1}^{N_1}V_{sk} - \sum_{h=1}^{N_2}V_{hk}\right)^2 \\
& + \frac{1}{2}\sum_{h=1}^{N_2}\beta_h\left[\sum_{k=1}^{M}t_k\left(q_{hk} - r_{hk}\right) - W_h\right]^2 \\
& + \sum_{k=1}^{M}\left(\sum_{s=1}^{N_1}\int_0^{V_{sk}} g^{-1}(V)dV + \sum_{h=1}^{N_2}\int_0^{V_{hk}} g^{-1}(V)dV\right)
\end{aligned} \tag{17}
$$

where $V_{\lambda k}$ and $V_{\gamma h}$ are the outputs of the multiplier neurons associated with power balance and water constraints, respectively; V_{hk} and V_{sk} are the outputs of continuous neurons hk, sk representing P_{hk}, P_{hk}, respectively.

The dynamics of the model for updating inputs of neurons are defined as follows:

$$
\begin{aligned}
\frac{dU_{sk}}{dt} & = -\frac{\partial E}{\partial V_{sk}} \\
& = -\left\{
\begin{aligned}
& t_k\left(b_s + 2c_s V_{sk}\right) \\
& + \left[V_{\lambda k} + \beta_k\begin{pmatrix} P_{Dk} + P_{Lk} \\ -\sum_{i=1}^{N_1}V_{ik} - \sum_{h=1}^{N_2}V_{hk}\end{pmatrix}\right]\left(\frac{\partial P_{Lk}}{\partial V_{sk}} - 1\right) + U_{sk}
\end{aligned}
\right\}
\end{aligned} \tag{18}
$$

$$
\begin{aligned}
\frac{dU_{hk}}{dt} & = -\frac{\partial E}{\partial V_{hk}} \\
& = -\left\{
\begin{aligned}
& \left[V_{\lambda k} + \beta_k\begin{pmatrix} P_{Dk} + P_{Lk} \\ -\sum_{s=1}^{N_1}V_{sk} - \sum_{j=1}^{N_2}V_{jk}\end{pmatrix}\right]\left(\frac{\partial P_{Lk}}{\partial V_{hk}} - 1\right) \\
& + \left[V_{\gamma h} + \beta_h\begin{pmatrix} \sum_{l=1}^{M}t_l\left(q_{lk} - r_{lk}\right) \\ -W_h\end{pmatrix}\right]\left(t_k\frac{\partial q_{hk}}{\partial V_{hk}}\right) + U_{hk}
\end{aligned}
\right\}
\end{aligned} \tag{19}
$$

$$\frac{dU_{\lambda k}}{dt} = +\frac{\partial E}{\partial V_{\lambda k}} = P_{Dk} + P_{Lk} - \sum_{s=1}^{N_1}V_{sk} - \sum_{h=1}^{N_2}V_{hk} \tag{20}$$

$$\frac{dU_{\gamma h}}{dt} = +\frac{\partial E}{\partial V_{\gamma h}} = \sum_{k=1}^{M}t_k\left(q_{hk} - r_{hk}\right) - W_h \tag{21}$$

where

$$\frac{\partial P_{Lk}}{\partial V_{sk}} = 2\sum_{i=1}^{N_1}B_{si}V_{ik} + 2\sum_{h=1}^{N_2}B_{sh}V_{hk} + B_{0s} \tag{22}$$

$$\frac{\partial P_{Lk}}{\partial V_{hk}} = 2\sum_{s}^{N_1}B_{hs}V_{sk} + 2\sum_{j=1}^{N_2}B_{hj}V_{jk} + B_{0h} \tag{23}$$

$$\frac{\partial q_{hk}}{\partial V_{hk}} = \left(b_h + 2c_h P_{hk}\right) \tag{24}$$

where B_{hj} and B_{si} are the loss coefficients related to hydro and thermal plants, respectively; B_{sh} and B_{hs} are the loss coefficients between thermal and hydro plants and $B_{sh}= B_{hs}^T$.

The algorithm for updating the inputs of neurons at step n is as follows:

$$U_{sk}^{(n)} = U_{sk}^{(n-1)} - \alpha_{sk}\frac{\partial E}{\partial V_{sk}} \tag{25}$$

$$U_{hk}^{(n)} = U_{hk}^{(n-1)} - \alpha_{hk}\frac{\partial E}{\partial V_{hk}} \tag{26}$$

$$U_{\lambda k}^{(n)} = U_{\lambda k}^{(n-1)} + \alpha_{\lambda k}\frac{\partial E}{\partial V_{\lambda k}} \tag{27}$$

$$U_{\gamma h}^{(n)} = U_{\gamma h}^{(n-1)} + \alpha_{\gamma h}\frac{\partial E}{\partial V_{\gamma h}} \tag{28}$$

where $U_{\lambda k}$ and $U_{\gamma h}$ are the inputs of the multiplier neurons; U_{sk} and U_{hk} are the inputs of the neurons sk and hk, respectively; $\alpha_{\lambda k}$ and $\alpha_{\gamma h}$ are step sizes for updating the inputs of multiplier neurons; and α_{sk} and α_{hk} are step sizes for updating the inputs of continuous neurons.

The outputs of continuous neurons representing power output of units are calculated by a sigmoid function:

$$V_{sk} = g(U_{sk}) = \left(P_s^{\max} - P_s^{\min}\right)\left(\frac{1 + \tanh\left(\sigma U_{sk}\right)}{2}\right) + P_s^{\min} \tag{29}$$

$$V_{hk} = g(U_{hk}) = \left(P_h^{\max} - P_h^{\min}\right)\left(\frac{1+\tanh\left(\sigma U_{hk}\right)}{2}\right) + P_h^{\min} \quad (30)$$

where σ is slope of sigmoid function that determines the shape of the sigmoid function [15].

The outputs of multiplier neurons are determined based on the transfer function as follows:

$$V_{\lambda k} = U_{\lambda k} \quad (31)$$

$$V_{\gamma h} = U_{\gamma h} \quad (32)$$

The proof of convergence for ALHN is given in [15].

3.1.1 Initialization

The algorithm of ALHN requires initial conditions for the inputs and outputs of all neurons. For the continuous neurons, their initial outputs are set to middle points between the limits:

$$V_{sk}^{(0)} = \left(P_s^{\max} + P_s^{\min}\right)/2 \quad (33)$$

$$V_{hk}^{(0)} = \left(P_h^{\max} + P_h^{\min}\right)/2 \quad (34)$$

where $V_{hk}^{(0)}$ and $V_{sk}^{(0)}$ are the initial output of continuous neurons *hk* and *sk*, respectively.

The initial outputs of the multiplier neurons are set to:

$$V_{\lambda k}^{(0)} = \frac{1}{N_1}\sum_{s=1}^{N_1}\frac{t_k\left(b_s + 2c_s V_{sk}^{(0)}\right)}{1 - \dfrac{\partial P_{Lk}}{\partial V_{sk}}} \quad (35)$$

$$V_{\gamma h}^{(0)} = \frac{1}{M}\sum_{k=1}^{M}\frac{V_{\lambda k}^{(0)}\left(1 - \dfrac{\partial P_{Lk}}{\partial V_{hk}}\right)}{t_k \dfrac{\partial q_{hk}}{\partial V_{hk}}} \quad (36)$$

The initial inputs of continuous neurons are calculated based on the obtained initial outputs of neurons via the inverse of the sigmoid function for the continuous neurons or the transfer function for the multiplier neurons.

3.1.2 Selection of parameters

By experiment, the value of σ is fixed at 100 for all test systems. The other parameters will vary depending on the data of the considered systems. For simplicity, the pairs of α_{sk} and α_{hk} as well as β_k and β_h can be equally chosen.

3.1.3 Termination criteria

The algorithm of ALHN will be terminated when either maximum error Err_{max} is lower than a predefined threshold ε or maximum number of iterations N_{max} is reached.

3.1.4 Overall procedure

The overall algorithm of the ALHN for finding an optimal solution for the HTS problem is as follows.

Step 1: Select parameters for the model in Section 3.1.2.
Step 2: Initialize inputs and outputs of all neurons using (33)-(36) as in Section 3.1.1.
Step 3: Set $n = 1$.
Step 4: Calculate dynamics of neurons using (18)-(21).
Step 5: Update inputs of neurons using (25)-(28).
Step 6: Calculate output of neurons using (29)-(32).
Step 7: Calculate errors as in section 3.1.3.
Step 8: If $Err_{max} > \varepsilon$ and $n < N_{max}$, $n = n + 1$ and return to Step 4. Otherwise, stop.

3.2 Best compromise solution by fuzzy-based mechanism

In a multi-objective problem, there often exists a conflict among the objectives. Therefore, finding the best compromise solution for a multi-objective problem is a very important task. To deal with this issue, a set of optimal non-dominated solutions known as Pareto-optimal solutions is found instead of only one optimal solution. The Pareto optimal front of a multi-objective problem provides decision makers several options for making decision. The best compromise solution will be determined from the obtained non-dominated optimal solution. In this paper, the best compromise solution from the Pareto-optimal front is found using fuzzy satisfying method [18]. The fuzzy goal is represented in linear membership function as follows:

$$\mu(F_j) = \begin{cases} 1 & \text{if} \quad F_j \le F_j^{\min} \\ \dfrac{F_j^{\max} - F_j}{F_j^{\max} - F_j^{\min}} & \text{if} \quad F_j^{\min} < F_j < F_j^{\max} \\ 0 & \text{if} \quad F_j \ge F_j^{\max} \end{cases} \quad (37)$$

where F_j is the value of objective *j* and F_{jmax} and F_{jmin} are maximum and minimum values of objective *j*, respectively.

For each *k* non-dominated solution, the membership function is normalized as follows [19]:

$$\mu_D^k = \sum_{i=1}^{Nobj}\mu(F_i^k) \Big/ \sum_{k=1}^{Np}\sum_{i=1}^{Nobj}\mu(F_i^k) \quad (38)$$

where μ^k_D is the cardinal priority of *k*th non-dominated solution; $\mu(F_j)$ is membership function of objective *j*; N_{obj} is number of objective functions; and N_p is number of Pareto-optimal solutions.

The solution that attains the maximum membership μ^k_D in the fuzzy set is chosen as the 'best' solution based on cardinal priority ranking:

$$\text{Max } \{\mu^k_D: k = 1, 2, \ldots, N_p\} \quad (39)$$

4. Numerical Results

The proposed ALHN based method has been tested on four hydrothermal systems. The algorithm of ALHN is implemented in Matlab 7.2 programming language and executed on an Intel 2.0 GHz PC. For termination criteria, the maximum tolerance ε is set to 10^{-5} for economic dispatch and emission dispatches and to 5×10^{-5} for determination of the best compromise solution.

4.1 Economic and emission dispatches

In this section, the proposed ALHN is tested on four systems. There are one thermal and one hydro power plants for the first system, one thermal and two hydropower plants for the second system, two thermal and two hydropower plants for the third systems, and two thermal and two hydropower plants for the fourth system. The data for the first three systems are from [1] and emission data from [20]. The data for the fourth system is from [2].

4.1.1 Case 1: The first three systems

For each system, the proposed ALHN is implemented to obtain the optimal solution for the cases of economic dispatch (w_1 = 1, w_2 = w_3 = w_4 = 0), emission dispatch (w_1 =0, w_2 = w_3 = w_4 =1/3), and the compromise case (w_1 = 0.5, w_2 = w_3 = w_4 = 0.5/3). The result comparisons for the three cases from the proposed ALHN with other methods including LGM, EPSO, and PM in [3] are given in Tables 1,

Table 1. Result comparison for the economic dispatch for first three systems (w_1 = 1, w_2 = w_3 = w_4 = 0)

System	Method	Fuel cost	Emission (kg)			CPU time
		($)	NO_x	SO_2	CO_2	(s)
1	LGM [3]	96,024.418	14,829.936	44,111.890	247,838.534	-
	EPSO [3]	96,024.607	14,830.001	44,111.984	247,839.504	-
	PM [3]	96,024.399	14,829.929	44,111.880	247,838.434	-
	ALHN	96,024.376	14,834.477	44,112.913	247,896.327	1.90
2	LGM [3]	848.241	575.402	4,986.155	2,951.455	-
	EPSO [3]	848.204	575.513	4,985.996	2,952.001	-
	PM [3]	847.908	575.477	4,985.743	2,951.649	-
	ALHN	848.349	575.261	4986.424	2950.185	0.91
3	LGM [3]	53,053.791	28,199.212	74,867.805	454,063.635	-
	EPSO [3]	53,053.793	28,199.206	74,867.802	454,063.559	-
	PM [3]	53,053.790	28,199.206	74,867.804	454,063.626	-
	ALHN	53,051.608	28,556.557	74,954.095	458,621.614	1.72

Table 2. Results comparison for the emission dispatch for first three problems (w_1 = 0, w_2 = w_3 = w_4 = 1/3)

Prob.	Method	Fuel cost	Emission (kg)				CPU time
		($)	NO_x	SO_2	CO_2	$NO_x+SO_2+CO_2$	(s)
1	LGM [3]	96,488.081	14,376.318	44,202.359	242,406.083	300,984.760	-
	EPSO [3]	96,488.384	14,376.405	44,202.506	242,407.419	300,986.330	-
	PM [3]	96,488.080	14,376.319	44,202.360	242,406.083	300,984.762	-
	ALHN	96,809.798	14,267.872	44,312.396	241,263.610	299,843.900	0.80
2	LGM [3]	851.983	571.991	4,993.746	2,922.820	8,488.557	-
	EPSO [3]	853.150	571.729	4,995.190	2,922.14	8,489.059	-
	PM [3]	851.981	571.992	4,993.747	2,922.820	8,488.559	-
	ALHN	851.905	572.003	4993.656	2922.810	8,488.469	1.68
3	LGM [3]	54,359.635	21,739.271	74,131.817	373,122.569	468,993.657	-
	EPSO [3]	54,359.657	21,739.270	74,131.817	373,122.568	468,993.655	-
	PM [3]	54,359.533	21,739.185	74,131.681	373,121.273	468,992.139	-
	ALHN	55,392.748	19,986.575	73,824.875	350,972.260	444,783.700	0.78

Table 3. Result comparison for the compromise case of three first systems (w_1 = 0.5, w_2 = w_3 = w_4 = 0.5/3)

Method		LGM [3]	EPSO [3]	PM [3]	ALHN
Total cost ($)	System 1	96,421.702	96,421.725	96,421.46	96,465.713
	System 2	851.208	851.079	852.388	850.065
	System 3	54,337.014	54,337.027	54,336.888	55,158.619
$NO_x+SO_2+CO_2$ (kg)	System 1	301,016.417	301,016.541	301,015.145	300,286.600
	System 2	8,488.928	8,487.872	8,489.438	8,490.776
	System 3	46,9025.136	46,9025.331	46,9023.262	44,5127.4
CPU time (s)	System 1	-	-	-	1.30
	System 2	-	-	-	1.53
	System 3	-	-	-	2.36

2, and 3. For the economic dispatch, the proposed ALHN can obtain better total costs than the other except for the system 2 which is slightly higher than the others. For the emission dispatch, the proposed ALHN can obtain less total emission than the others for all systems. In the compromise case, there is a trade-off between total cost and emission and the obtained solutions from the methods are non-dominated as in Table 3. The total computational times for economic dispatch, emission dispatch, and compromise case of the three systems from the proposed ALHN are compared to those from LGM, EPSO, and PM methods in [3]. As observed from the table, the proposed method is faster than the others for obtaining optimal solution. There is no computer reported for the methods in [3].

4.1.2 Case 2: The fourth system

For this system, each of the four objectives is individually optimized. The results obtained by the proposed ALHN for each case is given in Table 4. The minimum total cost and emission from the proposed ALHN is compared to those from BFA [2] in Table 5. In all cases, the proposed ALHN method can obtain better solution than BFA except for the case of CO_2 emission individual optimization.

Table 4. Total cost and emission for each individual objective minimization

	Min F_1 ($)	Min F_2 (kg)	Min F_3 (kg)	Min F_4 (kg)
F_1 ($)	**51891.414**	54294.526	53,104.125	54,221.820
F_2 (kg)	27443.038	**18,958.608**	20,822.202	18,963.243
F_3 (kg)	73381.146	72,416.895	**71,641.911**	72,358.568
F_4 (kg)	442113.211	335,810.130	357,415.390	**335,764.187**
CPU time(s)	1.29	1.53	1.79	1.11

Table 5. Result comparison for individual minimization of each objective

	BFA [2]	ALHN
Min F_1 ($)	52,753.291	51,891.414
Min F_2 (Kg)	19,932.248	18,958.608
Min F_3 (Kg)	71,988.754	71,641.911
Min F_4 (Kg)	334,231.219	335,764.187

4.2 Determination of the best compromise solution

In this section, the best compromise solution is determined for the first system in Section 4.1. For obtaining the best compromise solution for the system, three following cases are considered.

4.2.1 Case 1: Best compromise for two objectives

The best compromise solution for two objectives among the four objectives of this system is determined. The two objectives include the fuel cost and another emission objective while the other emission objectives are neglected. Therefore, there are three sub-cases for this combination including fuel cost and NO_x, fuel cost and SO_2, and fuel cost and CO_2. For each sub-case, 21 non-dominated solutions are obtained by ALHN to form a Pareto-optimal front and the best compromise solution is determined by the fuzzy based mechanism. The best compromise solution for each sub-case is given in Table 7. In this table, the best compromise solution for each sub-case is determined via the value of the membership function μ_D and the weight associated with each objective function is determined accordingly. For Sub-case 1, the best compromise solution is found at w_1 = 0.35 and w_2 = 0.65 corresponding to μ_D = 0.0547 at the solution number 14 among the 21 non-dominated solutions. The total fuel cost for this sub-case is $96,293.5771 with the total emission of 14,397.5374 kg NO_x. The Pareto-optimal front for this sub-case is given in Fig. 1. Fig. 2 depicts the methodology to determine the best compromise solution based on the relationship between membership function and the weight of objective. Similarly, the best compromise solution for Sub-case 2 and Sub-case 3 is determined in the same manner of Sub-case 1.

Table 6. Computational time comparison for the first three systems

Method	System 1	System 2	System 3
LGM [3]	14.83	11.46	12.26
EPSO [3]	95.36	83.73	105
PM [3]	43.44	39.27	49.01
ALHN	3.99	4.12	4.89

Table 7. The best compromise solutions for Case 1 with two objectives

	w_1	w_2	w_3	w_4	F_1 ($)	F_2 (kg)	F_3 (kg)	F_4 (kg)	μ_D
Sub-case 1	0.35	0.65	0	0	96,293.5771	14,397.5374	-	-	0.0547
Sub-case 2	0.35	0	0.65	0	96,038.9573	-	44,089.8723	-	0.0547
Sub-case 3	0.9	0	0	0.1	96,208.973	-	-	243,159.0661	0.059

Table 8. The best compromise solutions for Case 2 with three objectives

Sub-case	w_1	w_2	w_3	w_4	F_1 ($)	F_2 (kg)	F_3 (kg)	F_4 (kg)	μ_D
1	0.3	0.4	0.3	0	96174.9502	14479.9754	44094.8251	-	0.02518
2	0.6	0.2	0	0.2	96493.269	14320.319	-	241696.9	0.02494
3	0.7	0	0.2	0.1	96245.7307	-	44112.09	242856.6422	0.02591

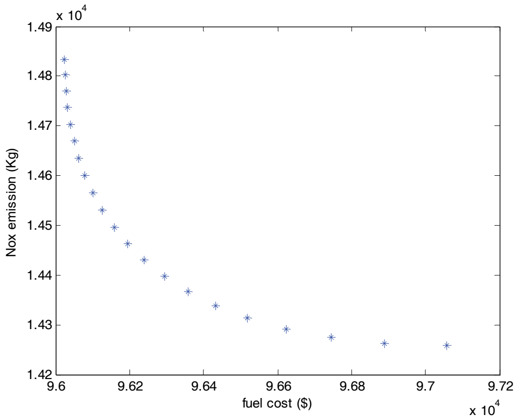

Fig. 1. Pareto-optimal front for fuel cost and NO_x emission in Sub-case 1 of Case 1

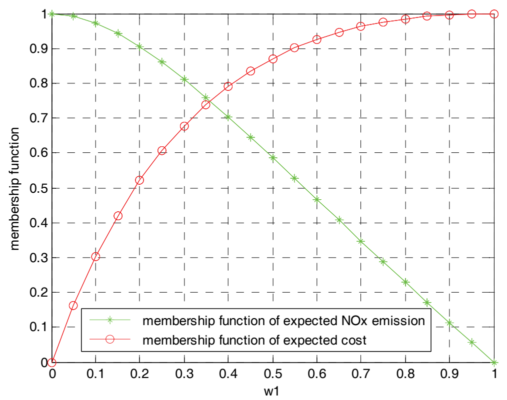

Fig. 2. Variation of membership functions against weight $w_2 = 1 - w_1$, $w_3 = w_4 = 0$ in Sub-case 1 of Case 1

4.2.2 Case 2: Best compromise for three objectives

The best compromise solution for three objectives among the four objectives is determined. The three objectives include the fuel cost and two other emission objectives among NO_x, SO_2, and CO_2. Therefore, there are three sub-cases considered for this case. Table 8 shows the best compromise solution for each sub-case with three objective functions with corresponding weight factors. For each sub-case, the best compromise solution is obtained based on the value of the membership function from different 43 non-dominated solutions.

4.2.3 Case 3: Best compromise for four objectives

The best compromise for all four objectives is considered in this section. The best compromise solution for this case is obtained from 284 non-dominated solutions based on the value of membership function μ_D given in Table 9.

The total computational times for the three cases above are given in Table 10. The total computational time here is the total time for calculation of all non-dominated solutions and determination of the best compromise solution. The total computational time for Case 1, Case 2, and Case 3 includes 21, 43, and 284 non-dominated solutions, respectively. Obviously, the computational time increases with the number of objective functions.

Table 9. The best compromise solutions for Case 3 with four objectives

Weight factor		Objective function		Membership function		μ_D
w_1	0.6	F_1 ($)	96,295.4624	$\mu(F_1)$	0.7376	0.00407
w_2	0.1	F_2(kg)	14,396.5261	$\mu(F_2)$	0.7599	
w_3	0.2	F_3 (kg)	44,126.2322	$\mu(F_3)$	0.8679	
w_4	0.1	F_4 (kg)	242,520.6672	$\mu(F_4)$	0.8092	

Table 10. Computational time for all test cases

Case		CPU (s)	No. solutions
Case 1: 2 objectives	1 (F_1, F_2)	34.18	21
	2 (F_1, F_3)	38.04	21
	3 (F_1, F_4)	24.25	21
Case 2: 3 objectives	1 (F_1, F_2, F_3)	64.99	43
	2 (F_1, F_2, F_4)	53.86	43
	3 (F_1, F_3, F_4)	54.23	43
Case 3: 4 objectives	(F_1, F_2, F_3, F_4)	311.97	284

5. Conclusion

In this paper, the proposed ALHN based method is effectively implemented for solving the multi-objective short-term fixed head hydro-thermal scheduling problem. ALHN is a continuous Hopfield neural network with its energy function based on augmented Lagrange function. The ALHN method can find an optimal solution for an optimization in a very fast manner. In the proposed method for solving the problem, the ALHN method is implemented for obtaining the optimal solutions for different cases and a fuzzy based mechanism is implemented for obtaining the best compromise solution. The effectiveness of the proposed method has been verified through four test systems with the obtained results compared to those from other methods. The result comparison has indicated that the proposed method can obtain better optimal solutions than other methods. Moreover, the proposed method has also implemented to determine the best compromise solutions for different cases. Therefore, the proposed ALHN method is an efficient solution method for solving multi-objective short-term fixed head hydro-thermal scheduling problem.

Nomenclature

a_{1s}, b_{1s}, c_{1s} Cost coefficients for thermal unit s,
a_h, b_h, c_h Water discharge coefficients for hydro unit h,
d_{1s}, e_{1s}, f_{1s} NO_x emission coefficients,
d_{2s}, e_{2s}, f_{2s} SO_2 emission coefficients,
d_{3s}, e_{3s}, f_{3s} CO_2 emission coefficients,
P_{Dk} Load demand of the system during subinterval k, in MW,
P_{hk} Generation output of hydro unit h during subinterval k,

in MW,

P_h^{min}, P_h^{max} Lower and upper generation limits of hydro unit *h*, in MW,

P_{Lk} Transmission loss of the system during subinterval *k*, in MW,

P_{sk} Generation output of thermal unit *s* during subinterval *k*, in MW,

P_s^{min}, P_s^{max} Lower and upper generation limits of thermal unit *s*, in MW,

q_{hk} Rate of water flow from hydro unit *h* in interval *k*, in acre-ft per hour or MCF per hour,

r_{hk} Reservoir inflow for hydro unit *h* in interval *k*, in acre-ft per hour or MCF per hour,

t_k Duration of subinterval *k*, in hours,

W_h Volume of water available for generation by hydro unit *h* during the scheduling period.

References

[1] A. H. A. Rashid and K. M. Nor, "An efficient method for optimal scheduling of fixed head hydro and thermal plants", *IEEE Trans. Power Systems*, vol. 6, no. 2, pp. 632-636, May 1991.

[2] I. A. Farhat and M. E. El-Hawary, "Multi-objective short-term hydro-thermal scheduling using bacterial foraging algorithm", *2011 IEEE Electrical Power and Energy Conference*, 176-181.

[3] J. Sasikala. M. Ramaswamy, "PSO based economic emission dispatch for fixed head hydrothermal systems", *Electr. Eng.*, vol. 94, no. 12, pp. 233-239, Dec. 2012

[4] A. J. Wood and B. F. Wollenberg, *Power generation, operation and control*, 2nd edn, New York: John Wiley & Sons, 1996.

[5] G.G. Oliveira and S. Soares, "A second-order network flow algorithm for hydrothermal scheduling," *IEEE Trans. Power Systems*, vol. 10, no. 3, pp. 1635-1641, Aug. 1995.

[6] Md.S. Salam, K.M. Nor, and A.R, Hamdan, "Hydrothermal scheduling based Lagrangian relaxation approach to hydrothermal coordination," *IEEE Trans. Power Systems*, vol. 13, no. 1, pp. 226-235, Feb. 1998.

[7] W.S. Sifuentes and A. Vargas, "Hydrothermal scheduling using benders decomposition: accelerating techniques," *IEEE Trans. Power Systems*, vol. 23, no. 3, pp. 1351-1359, Aug. 2007.

[8] K.P. Wong and Y.W. Wong, "Short-term hydrothermal scheduling - Part II: parallel simulated annealing approach," *IEE Proc.-Gener. Transm. Distrib.*, vol. 141, no. 5, pp. 502-506, Sept. 1994.

[9] P.-C. Yang, H.-T. Yang, and C.-L. Huang, "Scheduling short-term hydrothermal generation using evolutionary programming techniques," *IEE Proc.-Gener. Transnm. Distrib.*, vol. 143, no. 4, 371-376, Jul. 1996.

[10] E. Gil, J. Bustos, and H. Rudnick, "Short-term hydrothermal generation scheduling model using a genetic algorithm," *IEEE Trans. Power Systems*, vol. 18, no. 4, 1256-1264, Nov. 2003.

[11] L. Lakshminarasimman and S. Subramanian, "Short-term scheduling of hydrothermal power system with cascaded reservoirs by using modified differential evolution," *IEE Proc.-Gener. Transm. Distrib.*, vol. 153, no. 6, 693-700, Nov. 2006.

[12] J. Zhang, J. Wang, and C. Yue, "Small population-based particle swarm optimization for short-term hydrothermal scheduling," *IEEE Trans. Power Systems*, vol. 27, no. 1, 142-152, Feb. 2012.

[13] R. Naresh and J. Sharma, "Two-phase neural network based solution technique for short term hydrothermal scheduling," IEE Proc-Gener. Transm. Distrib., vol. 146, no. 6, 657-663, Nov. 1999.

[14] V. N. Dieu and W. Ongsakul, "Hopfield Lagrange for short-term hydrothermal scheduling," *IEEE Power Tech 2005*, June 2005, St. Petersburg, Russia.

[15] J.Polprasert and W.Ongsakul, "Augmented Lagrange Hopfield network for economic dispatch," *Australasian Universities Power Engineering Conference*, AUPEC 2007, Dec. 2007, Perth, Australia.

[16] V. N. Dieu and W. Ongsakul, "Enhanced merit order and augmented Lagrange Hopfield network for hydrothermal scheduling," *Int. J. Electrical Power & Energy Systems*, vol. 30, no. 2, pp. 93-101, Feb. 2008.

[17] V. N. Dieu and W. Ongsakul, "Improved merit order and augmented Lagrange Hopfield network for short term hydrothermal scheduling," *Energy Conversion and Management*, vol. 50, no. 12, pp. 3015-3023, Dec. 2009.

[18] M. Sakawa, H. Yano, and T. Yumine, "An interactive fuzzy satisfying method for multi-objective linear programming problems and its applications," *IEEE Trans. Systems, Man, and Cybernetics*, vol. SMC-17, no. 4, pp. 654-661, Jul./Aug. 1987.

[19] C.G. Tapia and B.A. Murtagh, "Interactive fuzzy programming with preference criteria in multi-objective decision making," *Computers & Operations Research*, vol. 18, no. 3, pp. 307-316, 1991.

[20] J.S. Dhillon, S.C. Parti and D.P. Kothari, "Fuzzy decision-making in stochastic multiobjective short-term hydrothermal scheduling," *IEE Proc. Gener., Transm. Distrib.*, vol. 149, pp. 191-200, 2002.

Thang Trung Nguyen received his B.Eng. and M.Eng. degrees in Electrical Engineering from University of Technical education Ho Chi Minh City (UTE), Ho Chi Minh city, Vietnam in 2008 and 2010, respectively. Now, he is teaching at department of electrical and electronics engineering, Ton Duc

Thang university and pursuing D.Eng. Degree at UTE, Ho Chi Minh city, Vietnam. His research interests include optimization of power system, power system operation and control and Renewable Energy.

Dieu Ngoc Vo received his B.Eng. and M.Eng. degrees in electrical engineering from Ho Chi Minh City University of Technology, Ho Chi Minh city, Vietnam, in 1995 and 2000, respectively and his D.Eng. degree in energy from Asian Institute of Technology (AIT), Pathumthani, Thailand in 2007. He is Research Associate at Energy Field of Study, AIT and lecturer at Department of Power Systems, Faculty of Electrical and Electronic Engineering, Ho Chi Minh City University of Technology, Ho Chi Minh city, Vietnam. His interests are applications of AI in power system optimization, power system operation and control, power system analysis, and power systems under deregulation.